A METHOD OF ION TEMPERATURE DETERMINATION WITH RETARDING POTENTIAL ANALYZER BY COMPUTER

Shigeyuki MINAMI, Shiro TSUTSUMI and Yoshio TAKEYA

Faculty of Engineering, Osaka City University, 3–138, Sugimoto 3-chome, Sumiyoshi-ku, Osaka 558

Abstract: We have been measuring the ion temperature by means of a retarding potential analyzer (RPA) aboard the sounding rocket whose velocity is comparable to the ion thermal velocity. In order to determine the ion temperature T_i from the RPA data, an optimum fitting procedure is used. It was believed that the deduction of T_i at low ram velocity by computer methods without assumption of ion mass number was impossible. This paper deals with an improved accurate fitting procedure to obtain T_i and mixed ion mass number. We advocate the usefulness of the improved error evaluation function. We also show the actual data analysis procedure.

1. Introduction

Retarding potential analyzer (RPA) is one of the ion temperature (T_i) probes which has some grids for energy analysis. The RPA's have been used with space vehicles to measure the drifted plasma. By the use of the differences of mass and energy with the same drift velocity, ion mass concentration can be obtained. Ion temperature measurement using RPA has been attempted by many workers (GRINGANZ and ZELIKMAN, 1957; HANSON and MCKIBBIN, 1961; HANSON *et al.*, 1970; GORDON, 1969; MCCLURE *et al.*, 1973; BENSON *et al.*, 1977).

The measurement of ion temperature by RPA on board satellites has been successful due to the large drift energy (1/3 eV/AMU). Since the RPA characteristic curves are usually so wide in energy, mass separation can be done easily. In the sounding rocket experiment, however, it is not easy to know the mass difference because the drift energy is very small. Although some RPA experiments aboard rockets had been done before satellites were used, ion temperature measurements were not available at altitudes less than 130 km. On the other hand, incoherent radars also provide reliable T_i in altitudes lower than 100 km (BENSON *et al.*, 1977). It may be likely that rocket RPAs are still potentially useful for ion temperature measurements compared with I. S. radar, since I. S. radar observation has poor time resolution.

The accurate measurement of T_i can be obtained by the RPA system with angle of attack measurements (MINAMI and TAKEYA, 1982; MINAMI *et al.*, 1982) and by the improved data analysis method which is described in this paper.

It is shown that the ion mass ratio which was assumed in the past data reduction (KNUDSEN and SHARP, 1965) can be deduced from the RPA characteristics even when the drift velocities of ions are comparable to the thermal velocities of ions. This method

needs two planer RPAs (MINAMI and TAKEYA, 1982), one is used for usual RPA and the other is used for the measurement of the angle of attack.

2. Theory of the RPA Voltage Current Characteristics

Typical RPA with a grid G for energy analysis and an ion collector C is illustrated in Fig. 1. Other grids for dc potential supply are not shown. Theoretical planer RPA collector current I_c is expressed by MINAMI and TAKEYA (1982) as

$$I_c=eN\eta\left\{\frac{v_0\cos\theta_a}{2}(1+\mathrm{erf}\,x)+\sqrt{\frac{KT_i}{2\pi m_i}}\right\}e^{-x^2}, \tag{1}$$

where

$$x=\sqrt{\frac{m}{2KT_i}}\left(v_0\cos\theta_a-\sqrt{\frac{2e}{m}V_R\sec^2\theta_a}\right), \tag{2}$$

V_R : retarding voltage
θ_a : angle of attack
T_i : ion temperature
m_i : ion mass
V_s : plasma potential to the reference electrode of vehicle
N_0 : plasma density
v_0 : velocity of vehicle.

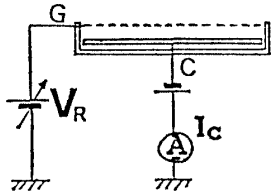

Fig. 1. A fundamental circuit of RPA.

And η which is a total transparency of the grids is calculated by comparing with other electron density probes.

Error function x is expressed as

$$\mathrm{erf}\,x=\int_x^\infty \exp(-y^2)\mathrm{d}y\,. \tag{3}$$

If two species of ions exist, ion mass ratio P is decided for NO^+ and O^+

$$P=\frac{N_{30}}{\text{total ion density }(N_{16}+N_{30})}, \tag{4}$$

where N_{30} and N_{16} are the partial ion density of NO^+ and O^+ respectively. The numerical calculations of eq. (1) are shown below.

In Fig. 2 examples of theoretical RPA characteristics for various values of T_i and three cases of P (0, 0.5, 1.0) are shown. Figure 3 shows theoretical RPA characteristics for various values of θ_a and three cases of P. Figure 4 shows examples of theoreti-

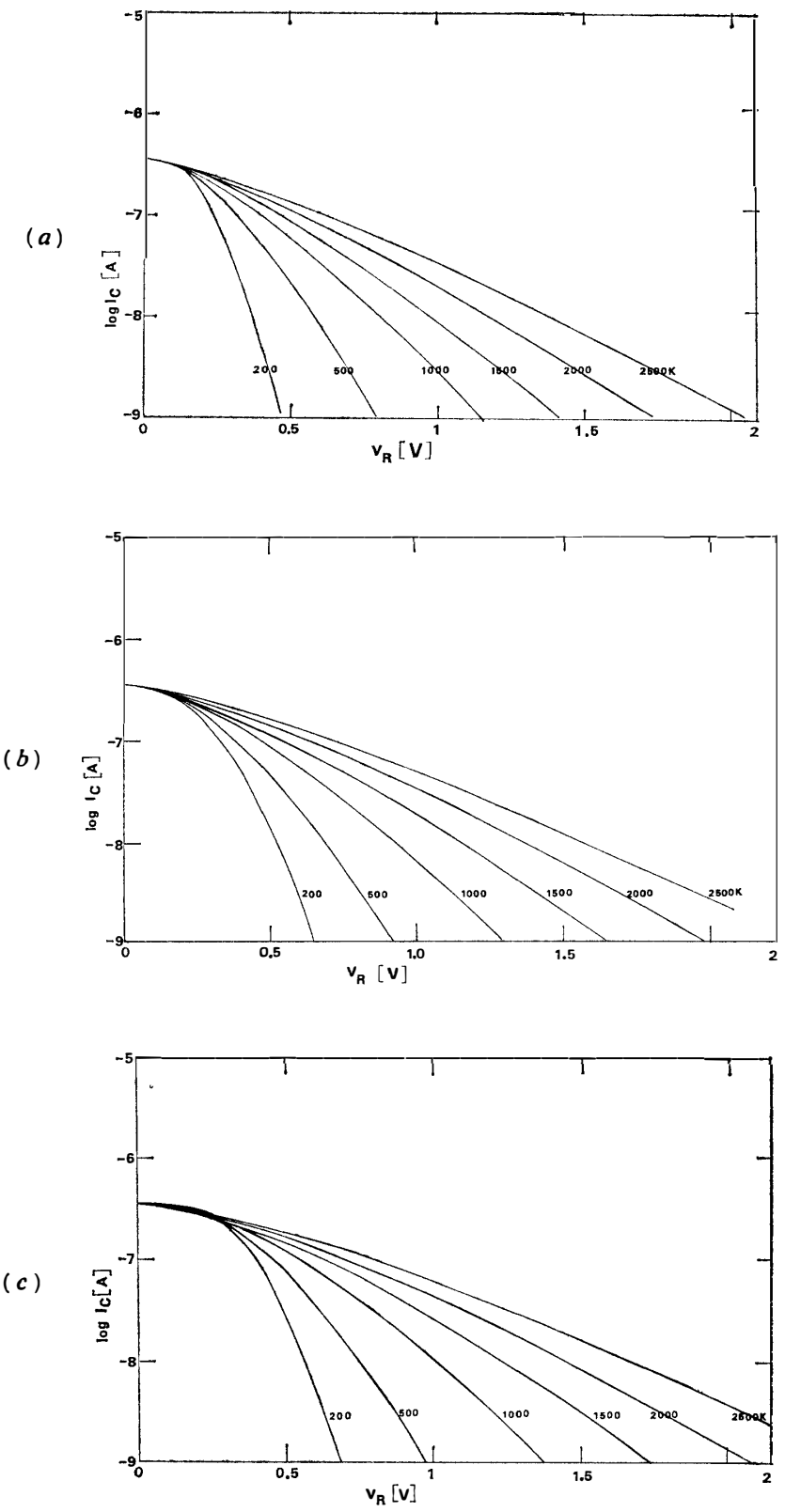

Fig. 2. The examples of theoretical RPA curves for various values of T_i; (a) $P=0$, (b) $P=0.5$ and (c) $P=1.0$, where $M=16$ AMU, $N_o=1.0\times10^6\,cm^{-3}$, $\theta_a=10°$, $v_o=1500\,m/s$, $S=57.6\,cm^2$ and $\eta=0.25$.

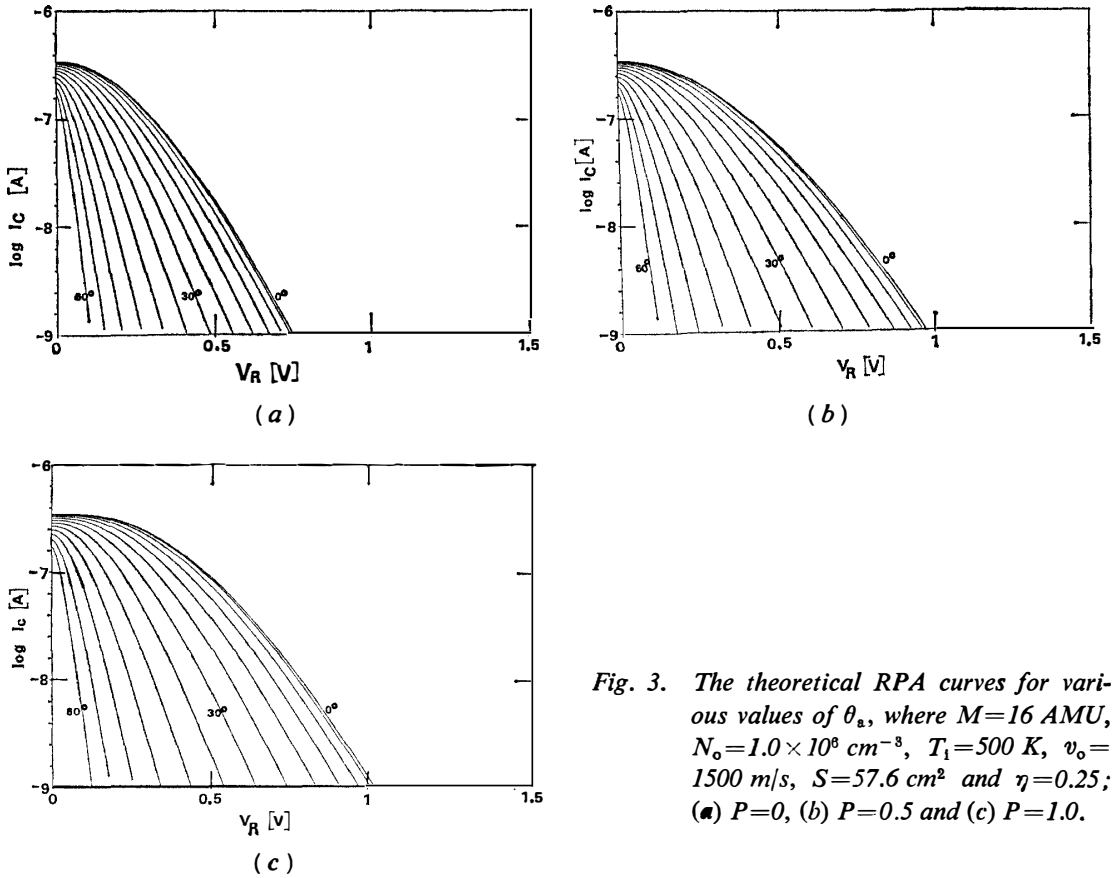

Fig. 3. The theoretical RPA curves for various values of θ_s, where $M=16$ AMU, $N_0=1.0\times10^6$ cm^{-3}, $T_i=500$ K, $v_0=1500$ m/s, $S=57.6$ cm^2 and $\eta=0.25$; (a) $P=0$, (b) $P=0.5$ and (c) $P=1.0$.

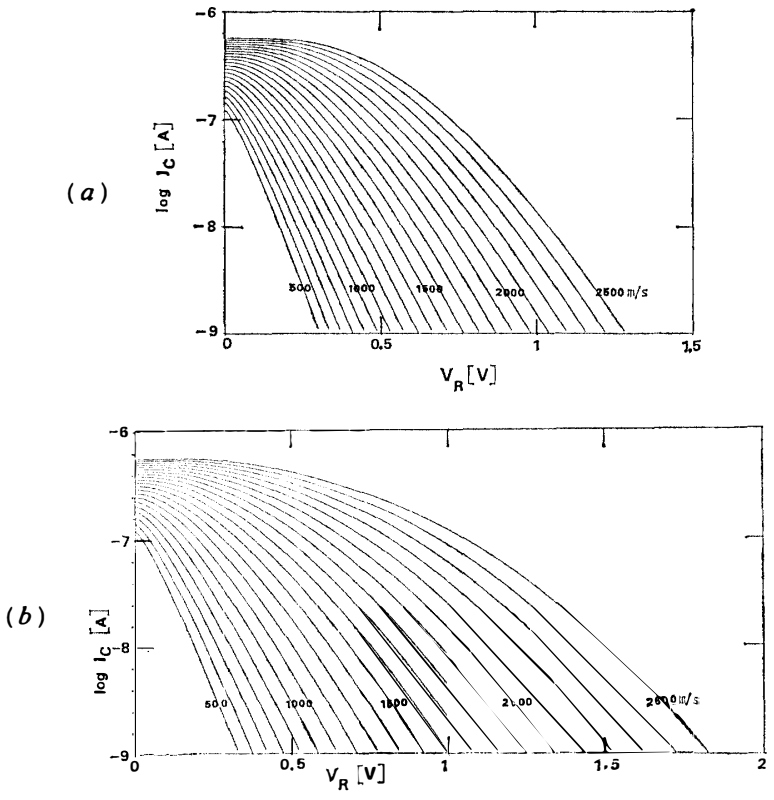

Fig. 4.

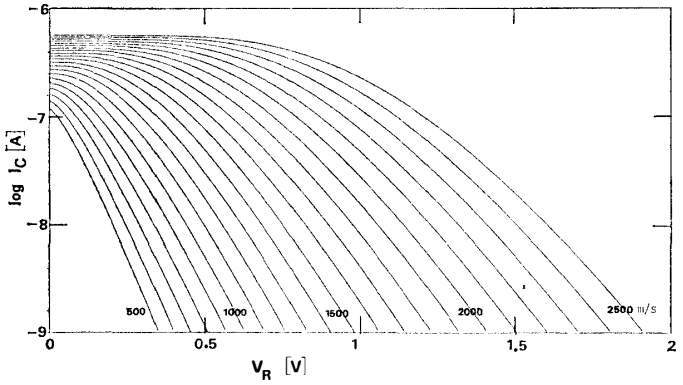

Fig. 4. The theoretical RPA curves for various values of velocity v_0, where total density $N_0=1.0\times 10^6$, $T_i=500$ K, $\theta_a=10°$, $S=57.6$ cm^2 and $\eta=0.25$; (a) $P=0$, (b) $P=0.5$ and (c) $P=1.0$.

cal RPA characteristics for various values of rocket velocity v_0 and three cases of P. These figures show that the difference of curves to the parameter P is not so clear as in the case when the velocity v_0 is very large.

Although the current reduction curves in Fig. 4 are very similar when v_0 is small, the gradients of the curves near the saturation region differ very much from each other. They contain the information about ion mass.

3. Data Analysis

Parameters are determined as follows:

(1) Vehicle velocity v_0 is decided from radar tracking data.

(2) The angle of attack θ_a between the normal direction of grid and the velocity vector of the vehicle is decided as referenced in a previous paper (MINAMI and TAKEYA, 1982).

(3) Plasma density N_0 is decided from the ion saturation current. Ion saturation current I_{is} does not depend on T_i, V_s, m_i as shown in Fig. 2. It depends only on N_0 and θ_a.

(4) T_i, m_i and V_s are derived using the optimum fitting procedure. By using the ion current data of RPA which is A-D converted, the plasma parameters T_i, m_i, P, V_s and the error evaluation function G are obtained by computer analysis. The experimental current data $J(V_i)$'s whose total sampling number is n are compared with the theoretical current $I(V_i)$'s which correspond to all sampling points V_i of V_R. The characteristic error evaluation function G

$$G=\sum_{i=1}^{n}\{\log J(V_i)-\log I(V_i)\}^2,$$

is used, which emphasizes the gradient of the curve. As the above theoretical curves show, information of ion temperature is contained not in the absolute current but in the gradient of the curve. We choose the same weight for every current.

There are the following three calculation loops for optimum fitting:

(1) The calculation loop of temperature T_i gives G under the assumed V_s, m_i, P.

(2) The calculation loop of potential V_s gives G under the assumed m_i and P.

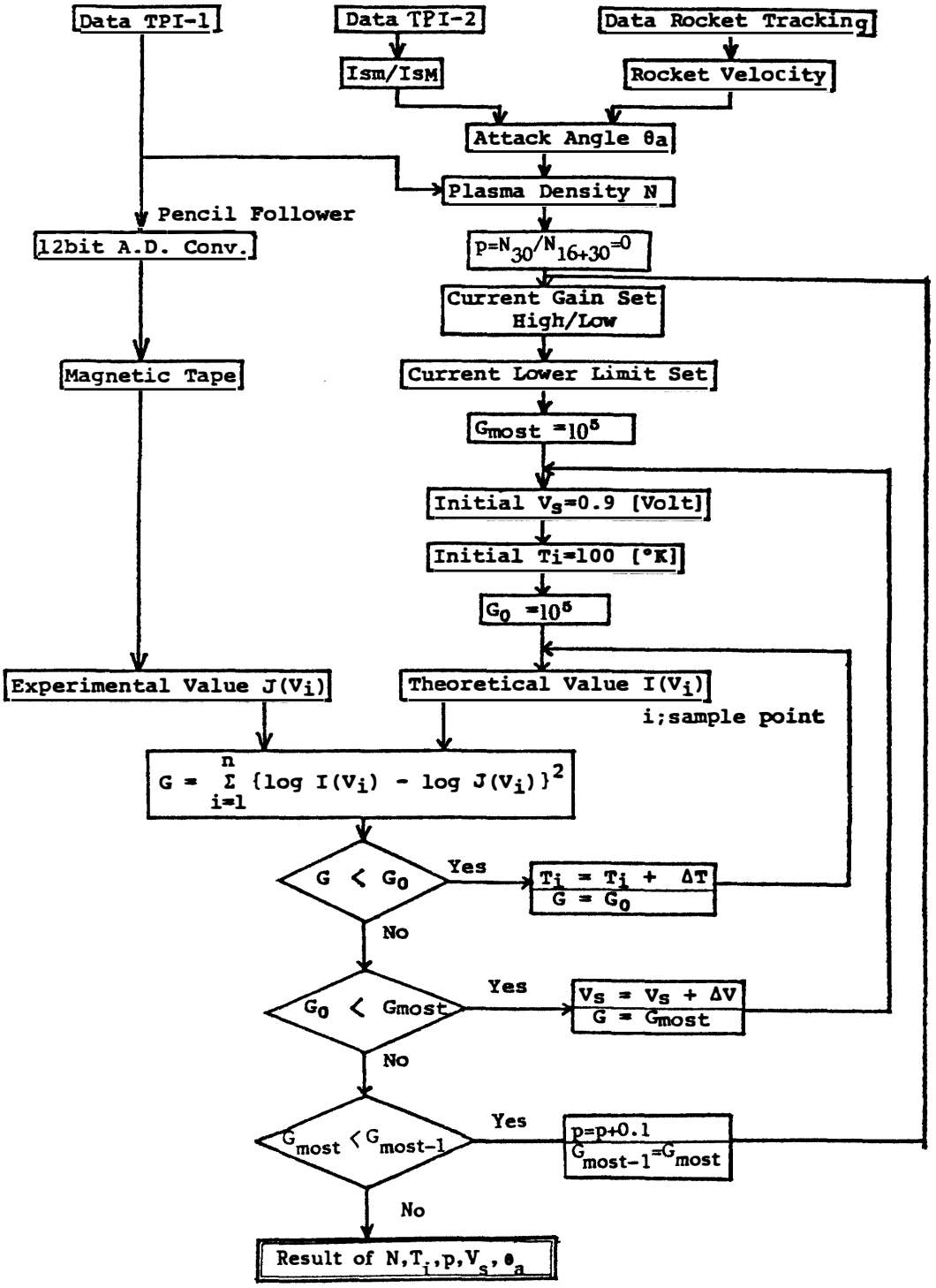

Fig. 5. Signal flow chart of the optimum fitting procedure.

(3) The calculation loop of ion mass gives G while varying ion mass ratio P. Through the above three calculation loops the most probable parameters of T_i, V_s, m_i and P are decided. In Fig. 5 the signal flow chart of numerical parameter calculation is illustrated.

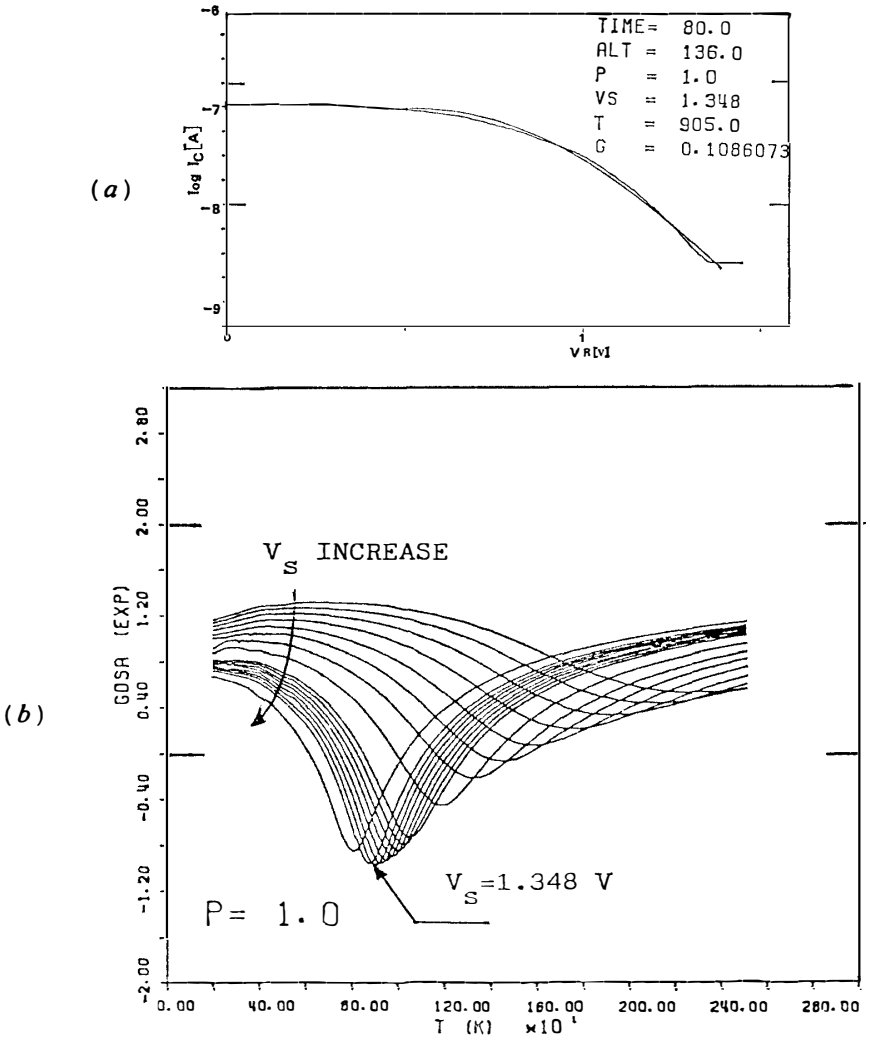

Fig. 6. An example of (a) fitted curve and (b) fitting process of G versus T_i (altitude 136 km).

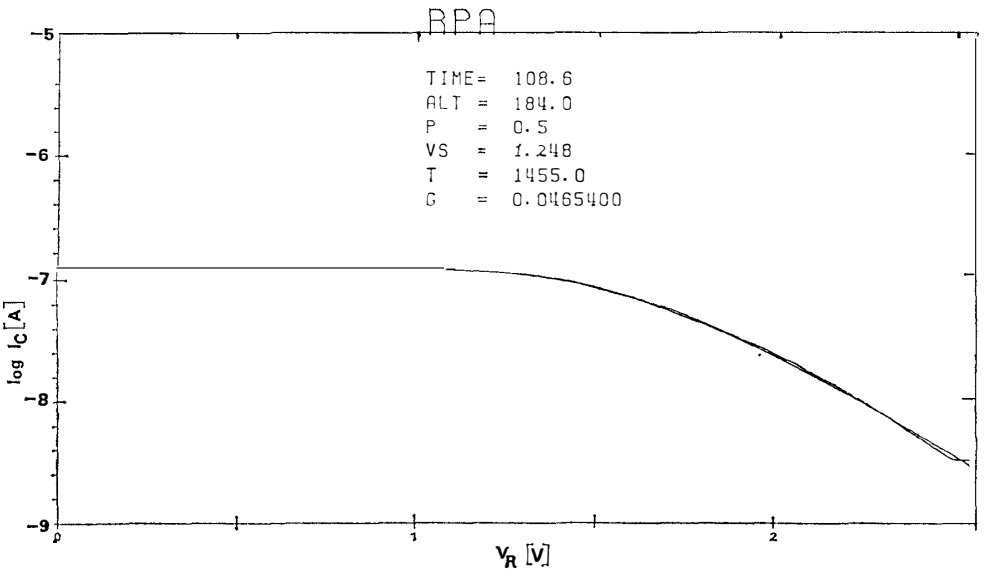

Fig. 7a.

4. An Example of Actual Data Analysis

This improved data analysis method was applied to the data obtained by K-9M-67 sounding rocket experiment. One RPA characteristic curve was obtained in about 0.3 s with the energy resolution of 0.007 eV.

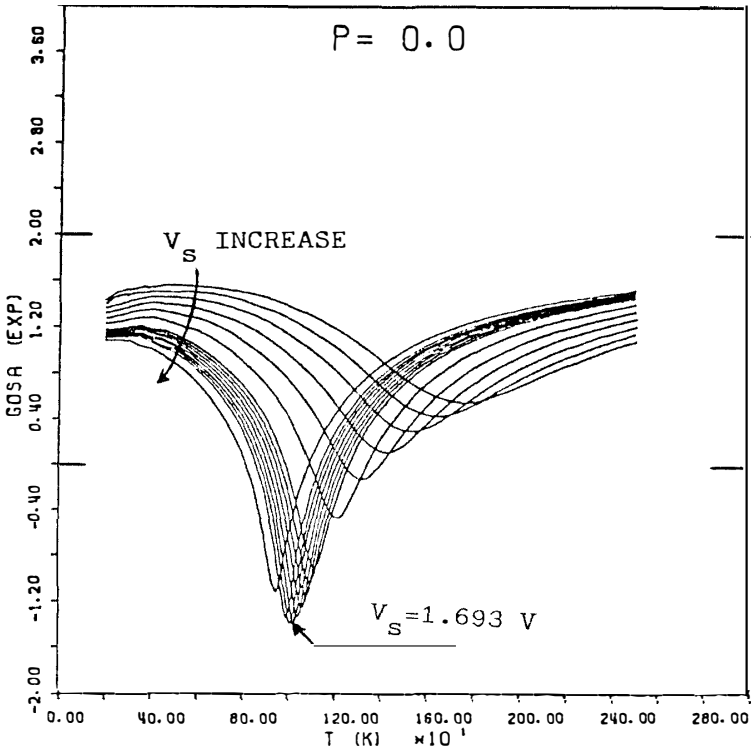

Fig. 7b.

Fig. 7. An example of (a) fitted curve and (b) fitting process of G versus T_i (altitude 229 km).

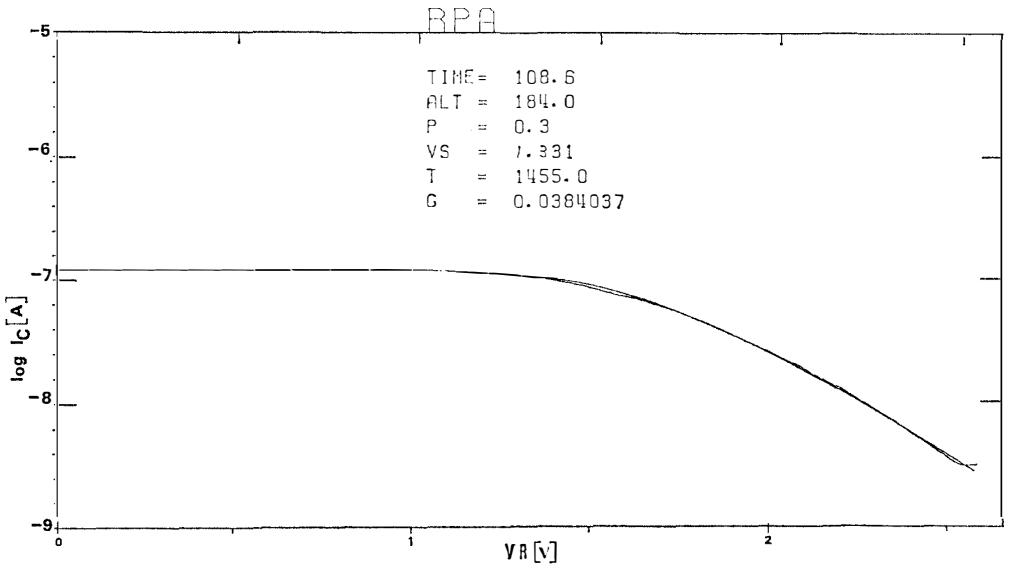

Fig. 8a.

As the signal flow chart shows, at first, step width of T_i and V_s loops are 50 K and about 60 mV respectively, finally T_i and V_s are decided with accuracy of 5 K and 7 mV respectively. In Fig. 6 the optimum fitted curves and experimental curve are illustrated. Figure 6b shows the fitting process of G *vs.* T_i for various values under fixed V_s. Ion temperature T_i is obtained from the minimum value of G. At this curve (altitude is 136 km) ion mass is assumed as NO^+ only from the well-known results of mass spectrometry (HOLMES *et al.*, 1965; SALAH, 1974). In Fig. 7 the optimum fitted curves and the process of fitting are drawn in the case of the measured altitude of 227 km.

The optimum fitting procedure including ion mass ratio loop must be done in an altitude range of 150 to 220 km. Figure 8 is an example of the fitting process for three

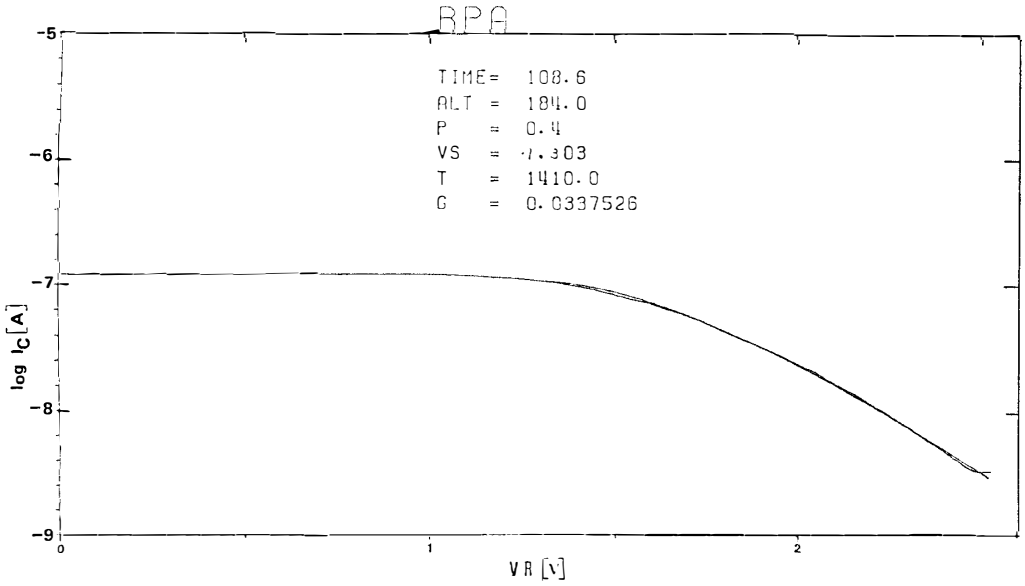

Fig. 8b.

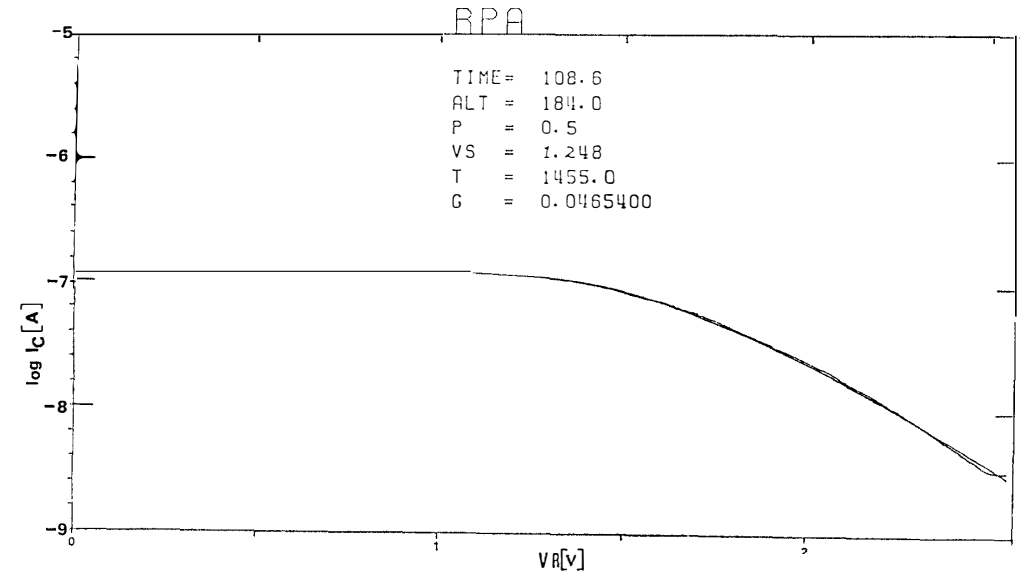

Fig. 8c.

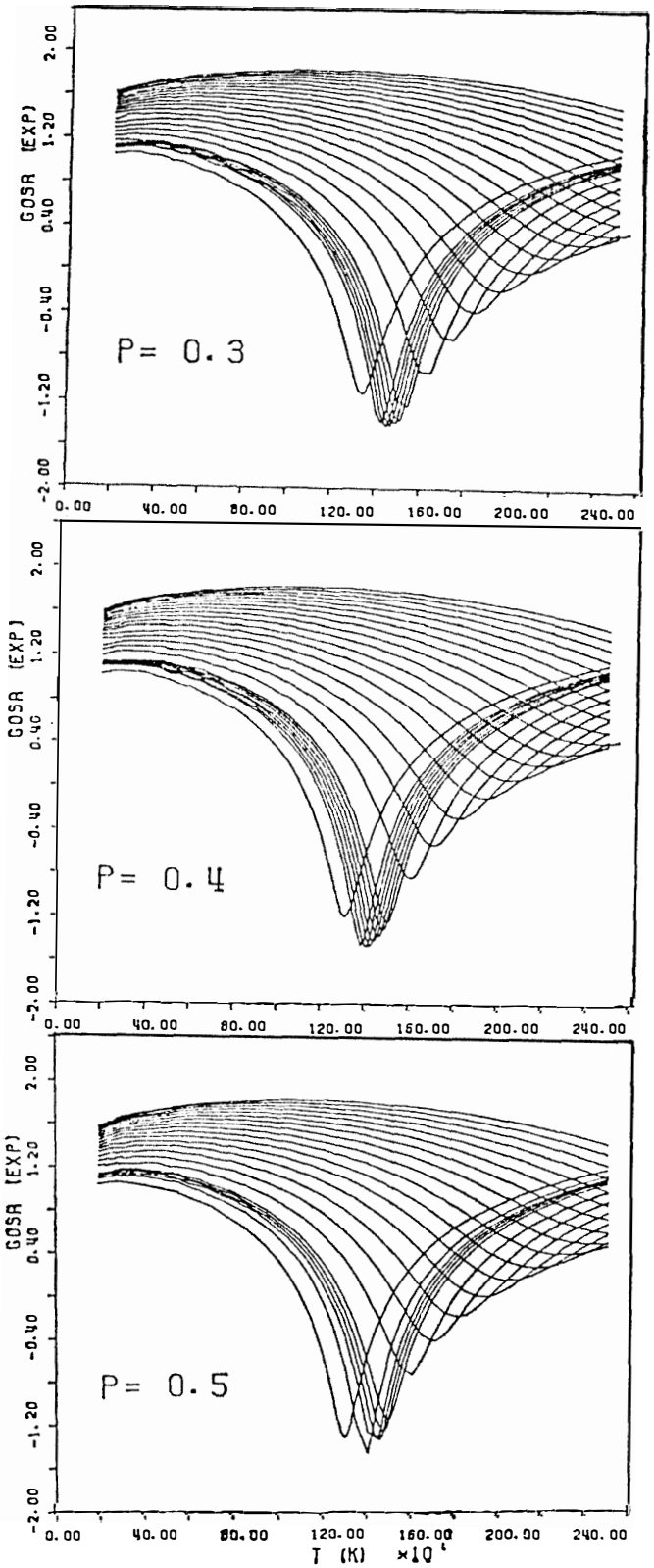

Fig. 8d.

Fig. 8. Optimum fitted curves and the fitting processes (a) P=0.3, (b) P=0.4, (c) P=0.5 and (d) fitting processes for various values of P.

values of P (0.3, 0.4, 0.5) at an altitude of 184 km. In Fig. 8d the fitting curves for the above three values are drawn. The comparison of each minimum G which is illustrated in the figures shows that the most probable parameter of P is 0.4.

These data are compared with the past experimental profiles of T_i and m_i. As a result, they are consistent with the well known geomagnetic data (MINAMI and TAKEYA, 1982).

5. Discussion

Because of an accurate RPA measurement system and the improved data analysis method described in this paper, accurate data of T_i and m_i by RPA aboard sounding

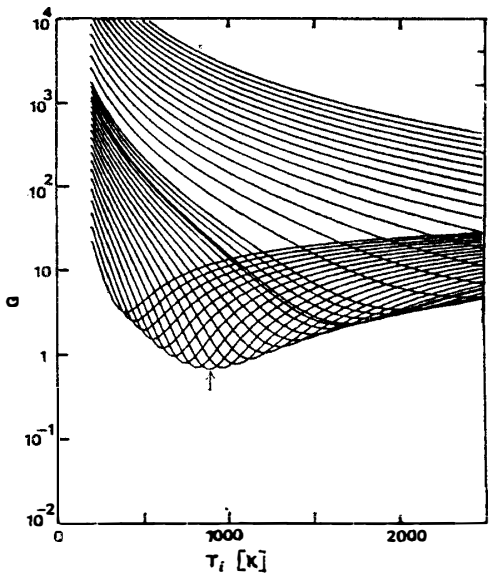

Fig. 9a.

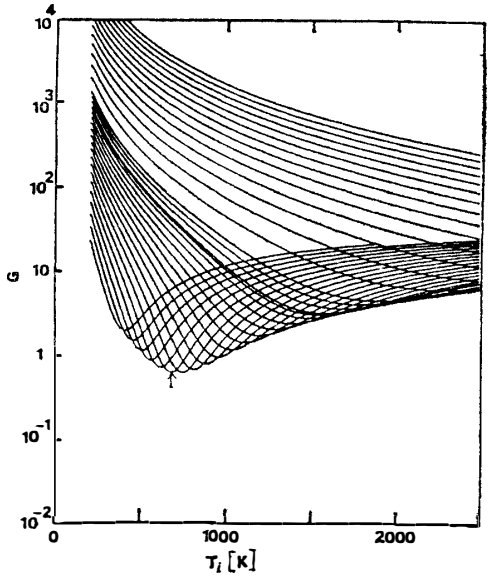

Fig. 9b.

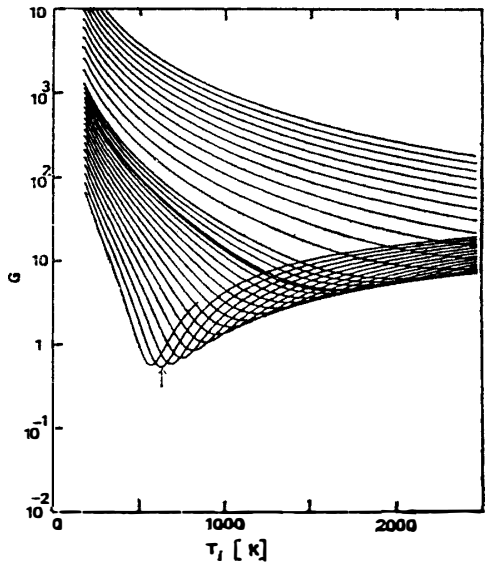

Fig. 9c.

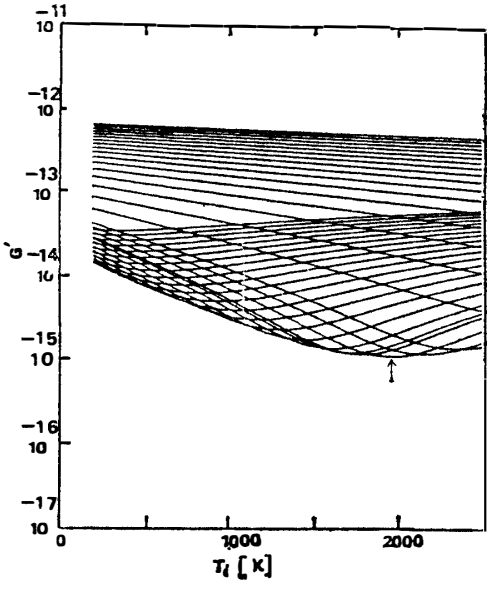

Fig. 9d.

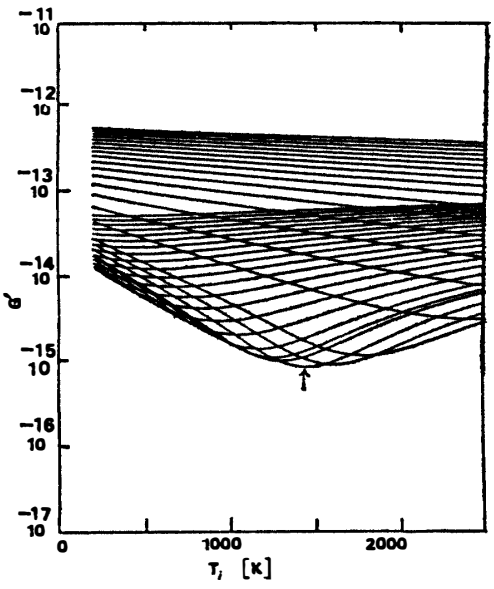

Fig. 9e.

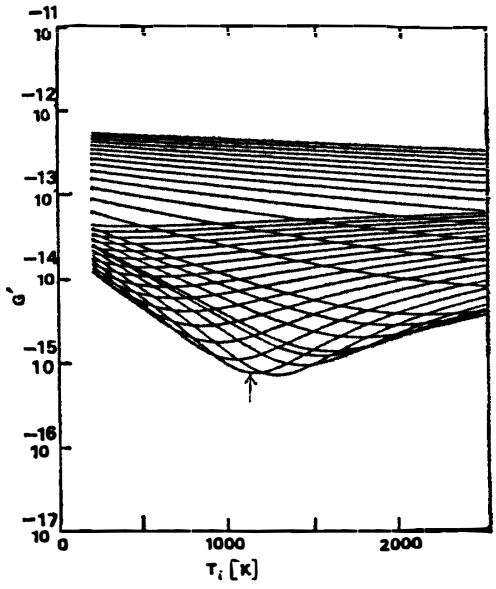

Fig. 9f.

Fig. 9. The example of the results of comparison between G and G′ for assumed values of P. The parameters of these curves are the assumed potential V_s.

rocket could be obtained. We used the improved evaluation function G which is effective in the slow drifting plasma.

We discuss the difference between this function G and the function G' of usual minimum square method. G' is expressed as

$$G' = \sum_{i=1}^{n} \{J(V_i) - I(V_i)\}^2 ,$$

(MOORE and ZEIGLER, 1960; MOSS and HYMAN, 1968; PATTERSON, 1969). Figure 9 shows the example of the result of comparison between G and G' for three assumed values of P. These results are obtained from the data at an altitude of 136 km. It is obvious that the minimum error by G' does not show the true temperature T_i. The ion saturation current curve sometimes shows the tilted distortion as a result of sheath expansion (MINAMI and TAKEYA, 1982). As function G' puts weight around the ion saturation region, data analysis using G' is much influenced by the ion saturation current. Therefore, it is thought that T_i obtained by G' contains the error due to distortion of ion saturation current. If the distortion in the ion saturation region exists, the difference of G and G' might be larger. On the other hand, RPA aboard satellites can escape such distortion at the saturation region because of comparably large input ion energy with the sheath potential V_s (HANSON *et al.*, 1970).

6. Conclusion

It was shown that an accurate deduction of T_i and m_i could be done by the use of the improved data analysis method from the RPA curve even in the slow drifting plasma (in sounding rocket experiment). Although the problem about this method is a long calculation time, it may be not so serious when more powerful computers become avail-

able.

This result motivates us to use RPA in the polar region to get the accurate measurement of the T_i profile which is useful to discuss thermodynamic behavior of the atmosphere by sounding rocket.

Acknowledgments

This study was done under the collaborating research programs of the Institute of Space and Astronautical Science, and the National Institute of Polar Research. The authors thank Mr. T. TSUJI for his assistence.

References

BENSON, R. F., BAUER, P., BRACE, L. H., CARLSON, H. C., HAGEN, J., HANSON, W. B., HOEGY, W. R., TORR, M. R., WAND, R. H. and WICKWAR, V. B. (1977): Electron and ion temperature, a comparison of ground-based incoherent scatter and AE-C satellite measurements. J. Geophys. Res., **82**, 36–42.

GORDON, L. W. (1969): The Langmuir plate and spherical ion probe experiments aboard Explorer XXXI. Proc. IEE, **57**, 1072–1077.

GRINGANZ, K. I. and ZELIKMAN, M. Kh. (1957): Measurements of the concentration of positive ions along the orbit of the artificial earth satellite Uzpekhi Fiz. Nauk, **63**, 239–252.

HANSON, W. B. and MCKIBBIN, D. D. (1961): An ion trap measurement of the ion concentration profile above the F_2 peak. J. Geophys. Res., **66**, 1667–1671.

HANSON, W. B., SANATANI, S., ZUCCARO, D. and FLOWERDAY, T. W. (1970): Plasma measurements with the retarding potential analyzer on Ogo 6. J. Geophys. Res., **75**, 5483–5501.

HOLMES, J. C., JOHNSON, C. Y. and YOUNG, J. M. (1965): Ionospheric chemistry. Space Res., **5**, 756–766.

KNUDSEN, W. C. and SHARP, G. W. (1965): Evidence for temperature stratification in the E region. J. Geophys. Res., **70**, 143–160.

MCCLURE, J. P., HANSON, W. B., NAGY, A. F., CICERONE, R. J., BRACE, L. H., BARAN, M., BAUER, P., CARLSON, H. C., EVANS, J. V., TAYLOR, G. N. and WOODMAN, R. F. (1973): Comparison of T_e and T_i from Ogo 6 and from various incoherent scatter radars. J. Geophys. Res., **78**, 197–205.

MINAMI, S. and TAKEYA, Y. (1982): Ion temperature determination in the ionosphere by retarding potential analyzer aboard sounding rocket. J. Geophys. Res., **87**, 713–730.

MINAMI, S., TSUTSUMI, S. and TAKEYA, Y. (1982): Graphical analysis method for a retarding potential analyzer and its application to the real-time measurements of ion temperature in space plasmas. Rev. Sci. Instrum., **53**, 1709–1713.

MOORE, R. H. and ZEIGLER, R. K. (1960): The solution of the general least-square problem with special reference to high speed computers. Los Alamos Sci. Lab. Rep. La-2367–1960.

MOSS, S. J. and HYMAN, E. (1968): Minimum variance technique for the analysis of ionospheric data acquired in satellite retarding potential analyzer experiments. J. Geophys. Res., **73**, 4315–4323.

PATTERSON, T. N. L. (1969): Deduction of ionospheric parameters from retarding potential analyzer. J. Geophys. Res., **74**, 4799–4801.

SALAH, J. E. (1974): Daily oscillation of the mid-latitude thermosphere studied by incoherent scatter at Millstone Hill. J. Atmos. Terr. Phys., **36**, 1891–1909.

(Received May 21, 1982; Revised manuscript received January 17, 1983)